Reversible Addition−Fragmentation Transfer Polymerization in Nanosized Micelles Formed in Situ

Genhua Zheng and Caiyuan Pan*

Department of Polymer Science and Engineering, University of Science and Technology of China, Hefei, Anhui, 230026, P. R. China

Received August 13, 2005; Revised Manuscript Received October 29, 2005

ABSTRACT: The reversible addition−fragmentation transfer (RAFT) polymerizations of 4-vinylpyridine (4VP) in tetrahydrofuran (THF) and in cyclohexane with RAFT agent, dithiobenzoate-terminated polystyrene (PS−SC(S)Ph), involve one polymerization rate (R_p = 0.083 mol L^{-1} h^{-1}) and two stages of polymerization (R_p = 0.164 and 0.0024 mol L^{-1} h^{-1} before and after 5 h), respectively. The polymerization of 4VP and divinylbenzene (less than 10% relative to 4VP) in THF led to gelation, but the polymerization in cyclohexane displayed clear solution consistently throughout polymerization, and kinetic studies showed sudden decrease of polymerization rate and sharp increase of molecular weight at around 5 h. Polymerization was followed by gel permeation chromatography (GPC) and the combination of GPC and multiangle laser light scattering (MALLS). The results show the formation of micelles with PS as shell and poly(PVP-*co*-DVB) as core by microphase separation; the micelles' size increased fast around 5 h polymerization, and then the micelles grew slowly with progress of polymerization. A series of experiments were made to look for reasons for the decrease of polymerization rate at around 5 h of polymerization, and the possible reasons are the restriction of diffusion and higher concentration of dithiobenzoate groups in the cores of micelles. The effects of molecular weight of RAFT agent and the content of DVB in the mixture of 4VP and DVB on the polymerization and the formation of micelles were also investigated. ^{1}H NMR, dynamic and static light scattering (DLS, SLS), transmission electron micrograph (TEM), and atomic force microscopy (AFM) were used to characterize the micelles, and the micelles with less than 50 nm in diameter and narrow size distribution were obtained. Thus, an efficient synthetic method of stable micelles was developed in comparison with the self-assembling of block and graft polymers in selective solvents, and one advantage of this method is that the polymerization, micellization, and cross-linking reactions occur in one pot, forming stable, narrow micelles with functional cores.

Introduction

Star-shaped polymers have received significant attention over the past decades because of their unique three-dimensional shape and highly branched structure.[1] Therefore, various methods of preparing the star-shaped polymers have been developed.[2] Among those synthetic methods based on living polymerizations, the controlled radical polymerizations of cross-linkable monomers initiated by reactive linear polymer chains (arm-first) can produce the largest arm number of star polymers.[3−6] In those polymerizations higher contents of cross-linkable monomers are generally used.[7,8] An appropriate feed ratio of monomer to cross-linkable compound is an important factor for successful synthesis of the star-shaped polymers; a lower feed ratio of divinylbenzene (DVB) to styrene (St) will lead to gelation generally.[6] Most of the micelles are prepared by self-assembling of block and graft copolymers in selective solvents,[9,10] but they are sensitive to the environment, such as solvents, concentration, and temperature. Therefore, extensive studies have been made to stabilize micelles by cross-linking the core or the shell of micelles during the past two decades,[11,12] since they have potential applications, such as in catalysis, biological or biomedical fields, electronic, and optical devices.[13−16] The star (hairy) polymers and the micelles can be identified by the relative length of the core and the corona blocks.[17] If the nanosized micelles can be prepared by arm-first method via controlled radical block copolymerizations with lower feed ratio of cross-linkable compound to monomer, this will provide a facile one-pot synthetic route to stable micelles. The challenge is how to avoid gelation during the polymerization.

Using poly(ethylene glycol) (PEG) and ammonium cerium(IV) nitrate as redox initiation system, the aqueous polymerization of *N*-isopropylacrylamide (NIPAAm) above the lower critical solution temperature (LCST) formed the micelles,[18,19] but no kinetic study and more polymerization mechanism evidences were provided. If micelles are formed by microphase separation at early stage of polymerization, gelation of polymerization systems might be avoided. Since poly(vinylpyridine) can form complexes with various metal ions,[20−22] the nanosized noble metal or bimetal cluster encapsulated in micelles might be used as homogeneous catalysts. The polystyrene (PS) can dissolve in Θ solvent, cyclohexane, at higher temperature and precipitated at lower temperature. This property will provide an easy recycling method of the catalyst. In this article, we report our investigation on the RAFT copolymerization of 4VP and DVB in a selective solvent using dithiobenzoate-terminated PS as RAFT agent, and the formation and characterization of the micelles were studied.

Experimental Section

Materials. THF was refluxed over sodium for 24 h and then distilled prior to use. St (Shanghai Chemical Reagent Co, 99%) and 4VP (Acros, 96%) were dried over CaH_2 and distilled under reduced pressure prior to use. DVB (50%, mixture of isomers, Shanghai Chemical Reagent Co.) was purified by passing it through the silica gel column. The 2,2′-azobis(isobutyronitrile) (AIBN) was purified by recrystallization from ethanol. Ethyl 2-bromoisobutyrate (Aldrich, 98%) and all other reagents with analytical grade were used as received.

* Corresponding author: Ph 86-551-3603264; Fax 86-551-3601592; e-mail pcy@ustc.edu.cn.

10.1021/ma0517897 CCC: $33.50
Published on Web 12/02/2005

Table 1. Preparation Conditions and Results of PS−SC(S)Ph

	feed molar ratio[a]								
	St[a]	ECPDB[a]	AIBN[a]	T (°C)	time (h)	conv[b] (%)	$M_{n,NMR}$[c] (g mol^{-1})	$M_{n,GPC}$[d] (g mol^{-1})	M_w/M_n[d]
PS1	500	10	1	110	6	42	2460	2000	1.11
PS2	600	10	1	110	6	58	3370	2840	1.05
PS3	1200	10	1	110	8	54	6320	6040	1.06
PS4	1600	10	1	110	8.5	47	8740	8440	1.03
PS5	2000	10	1	110	9	50	11200	11000	1.03

[a] St = styrene; ECPDB = 2-(ethoxycarbonyl)-2-propyl dithiobenzoate; AIBN = 2,2′-azobis(isobutyronitrile). [b] Conversions were calculated gravimetrically. [c] Based on ^{1}H NMR data, the number-average molecular weight of PS, $M_{n,PS}$ (NMR) was calculated according to $M_{n,PS}$ (NMR) = $(2I_{7.32-6.30}/5I_{7.85}) \times 104 + 268$, where $I_{7.32-6.30}$ and $I_{7.85}$ are integral values of the signals at δ = 7.32−6.30 and 7.85 ppm; 104 and 268 are molecular weights of S and ECPDB. [d] The number-average molecular weight ($M_{n,GPC}$) and molecular weight distribution (M_w/M_n) were obtained from GPC measurements.

Synthesis of 2-(Ethoxycarbonyl)-2-propyl Dithiobenzoate (ECPDB). The chain transfer agent ECPDB was prepared as follows. Magnesium (2.00 g, 0.083 mol) and 80 mL of dry THF were added into a 250 mL three-necked flask, and then bromobenzene (15.7 g, 0.1 mol) was added dropwise into the reaction mixture over 0.5 h. The reaction was carried out at 40 °C until complete disappearance of magnesium. Then, carbon disulfide (7.62 g, 0.1 mol) was dropped over about 20 min. After reaction proceeded at 40 °C for 4 h, ethyl 2-bromoisobutyrate (17.5 g, 0.09 mol) was added. The reaction was carried out at 90 °C for 60 h. After slow addition of 100 mL of ice water into the reaction mixture, the aqueous phase was extracted with CS_2 (3 × 50 mL). The organic extracts were combined. The combined extracts were washed with water and then dried over anhydrous magnesium sulfate. After removing the solvent by rotating evaporator, the product obtained was purified by silica column chromatography using petroleum ether/diethyl ether (10/1 v/v) as the eluent. After the solvent was removed under reduced pressure, ECPDB was obtained as a red oil (10.52 g, yield 49.2%).

^{1}H NMR (300 MHz, $CDCl_3$), δ (TMS, ppm): 1.24 (t, 3H, CH_2CH_3), 1.76 (s, 6H, 2 × CH_3), 4.17 (q, 2H, OCH_2CH_3), 7.35 (dd, 2H, m-Ar*H*), 7.52 (dd, 1H, *p*-Ar*H*), 7.95 (d, 2H, *o*-Ar*H*).

Preparation of Dithiobenzoate-Terminated Polystyrene (PS−SC(S)Ph). The general procedure is as follows. The St (24 g, 0.23 mol), ECPDB (0.312 g, 1.2 mmol), and AIBN (20 mg, 0.12 mmol) were added into a 50 mL polymerization tube with magnetic bar. After three freeze−evacuate−thaw cycles, the tube was sealed under high vacuum and then placed in an oil bath preheated at 110 °C while stirring. After 9 h, the tube was cooled to room temperature with ice−water and then opened. The polymer was precipitated by pouring a polymer solution in THF into excess methanol while stirring. The precipitate obtained by filtration was dried in a vacuum oven at room temperature overnight. The PS−SC(S)Ph was obtained in 50% yield; M_n(GPC) = 11 000 and M_w/M_n = 1.03.

RAFT Block Polymerizations of 4VP with PS−SC(S)Ph as Macro-RAFT Agent in Cyclohexane and in THF. In a typical experiment, PS−SC(S)Ph (PS2 in Table 1, 3.6 g, 1.2 mmol), 4VP (7.2 g, 72 mmol), and AIBN (18 mg) were mixed and then divided equally into six portions. Each portion was added into a 20 mL glass tube. After addition of 5 mL of cyclohexane (or 5 mL of THF), the mixture was degassed by three freeze−evacuate−thaw cycles. The tube was sealed under vacuum and then placed into an oil bath thermostated at 90 °C. The polymerization tubes were taken out at the prescribed time intervals, and then they were put into ice water for stopping the polymerization. After cooled to room temperature, the tubes were opened. The polymerization mixtures were poured into an excess of petroleum ether while stirring. The precipitates were collected by filtration and then dried at 40 °C in a vacuum oven overnight. The conversion of 4VP was calculated on the basis of the amount of polymers obtained and their ^{1}H NMR data.

RAFT Copolymerization of 4VP and DVB in Cyclohexane with PS−SC(S)Ph as Macro-RAFT Agent and AIBN as Initiator. After 4VP, DVB, PS−SC(S)Ph, and AIBN were mixed homogeneously, the solution was divided equally into eight portions. Each portion contained 0.6 g of PS−SC(S)Ph (PS2, 0.2 mmol), 1.2 g of 4VP (12 mmol), 0.12 g of DVB (content: 50%, 0.39 mmol), and 3 mg of AIBN. Those eight portions were added into eight 20 mL glass tubes separately. After 5 mL of cyclohexane was added into each tube, the mixture was degassed by three freeze−evacuate−thaw cycles. The tubes were sealed under vacuum and then placed into an oil bath thermostated at 90 °C. The polymerization tubes were taken out, and the polymerization was stopped by putting the tube into ice water at 0.5, 1, 2, 3, 4, 5, 10, and 20 h polymerizations. After cooled to room temperature, the tube was opened. The polymerization mixture was poured into an excess of petroleum ether while stirring. The precipitate was collected by filtration and dried at 40 °C in a vacuum oven overnight. The conversion of 4VP was measured on the basis of the amount of polymers obtained and ^{1}H NMR data.

Characterization. Transmission electron micrograph (TEM) observations were performed with a Philips CM30 microscope at an accelerating voltage of 120 kV. The samples for TEM observation were prepared by depositing a drop of the polymer solution in THF on copper grids. Atomic force microscopy (AFM) observation was performed on DI Nanoscopy IIIa with tapping mode, and the AFM images were obtained at room temperature in air. Samples for AFM imaging were prepared by placing 10 μL sample solution in THF (2 × 10^{-3} wt %) onto freshly cleaved mica and then spin-coated at 1000 rpm for 3 min at room temperature. The ^{1}H NMR (300 MHz) measurements were performed on Bruker DMX300 spectrometer in $CDCl_3$ using tetramethylsilane as an internal reference. FT-IR spectra were recorded on a Vector-22 FT-IR instrument. The molecular weight and polydispersity indexes were determined on a Waters 150C gel permeation chromatography (GPC) equipped with three ultrastyragel columns (500, 10^3, 10^4 Å) in series and RI detector at 30 °C, using monodispersed polystyrene as calibration standard. THF was used as eluent at a flow rate of 1.0 mL/min. Combined GPC and multiangle laser light scattering (MALLS) analysis was carried out at 30 °C to determine size of the micelles in THF. A dual-detector system, consisting of a multiangle laser light scattering device and a differential refractometer (λ = 690 nm), was used. The GPC system (Waters 2690D) was equipped with Shodex K803 columns. THF was used as eluent at flow rate of 1 mL/min. The polymer concentration was 3 mg/mL. The MALLS (DAWN DSP, Wyatt Technology Co., 30 mW) detector was operated at a laser wavelength of 690 nm.

Laser light scattering (LLS) studies were conducted with a modified commercial LLS spectrometer (ALV/SP-125) equipped with an ALV-5000 multi-τ digital time correlator and a solid-state laser (ADLAS DPY42511, out power was ~400 mW at λ = 532 nm) at a fixed scattering angle (θ) of 15° with both cumulants and CONTIN software. The dn/dc of the PS_{36}/$P4VP_{33}$ micelles was determined to be 0.168 in THF solution at 20 °C while PS_{117}/$P4VP_{37}$ was 0.180. Static light scattering (SLS) studies were conducted at 25 °C using the same instrument at scattering angles ranging from 15° to 135°. The weight-average molecular weight (M_w) and radius of gyration (R_g) data were obtained using standard Zimm plot analyses.

Results and Discussion

Investigation on RAFT polymerization of styrene has evidenced its living nature.[23,24] The macro-RAFT agent PS−SC-

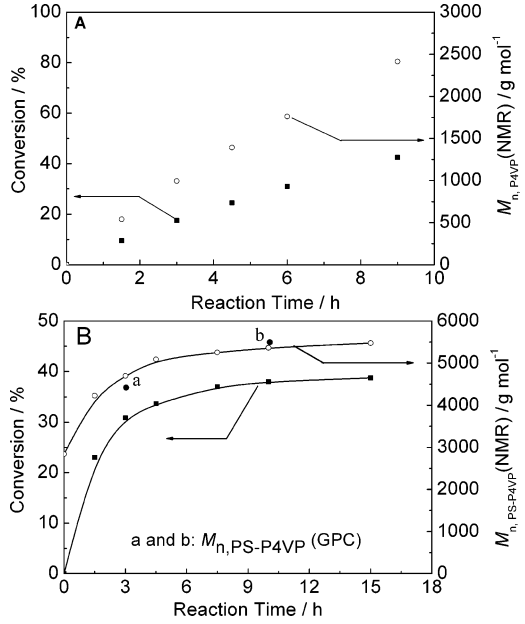

Figure 1. Evolution of conversion of 4-vinylpyridine (4VP) and the number-average molecular weight of the P4VP block based on ^{1}H NMR data, $M_{n,P4VP}$(NMR), with polymerization time for the block copolymerization of 4VP with macro reversible addition−fragmentation transfer agent, PS−SC(S)Ph, in tetrahydrofuran (A) and in cyclohexane (B), respectively. Feed molar ratio: PS−SC(S)Ph(PS2 in Table 1)/4VP/AIBN = 11/654/1; THF or cyclohexane: 5 mL; temperature: 90 °C.

(S)Ph used in this study was also prepared by RAFT polymerization of St using ECPDB as RAFT agent and AIBN as initiator. The conditions and results are listed in Table 1. The results show that the molecular weight can be controlled by the feed ratio of monomer to ECPDB and conversion. The molecular weight distribution of the polymers obtained is quite narrow.

Comparison of the Block Copolymerizations of 4VP and St in Different Solvent. In the investigation on synthesis of star-shaped polymers via RAFT polymerization,[25] we observed a very interesting phenomenon, and the RAFT polymerizations with the same feed ratio and conditions in THF and in cyclohexane demonstrated different kinetics behaviors (Figure 1). Figure 1A shows that the 4VP conversion increases almost linearly with polymerization time, and the polymerization rate (R_p) is 0.083 mol L^{-1} h^{-1} for the polymerization of 4VP using PS−SC(S)Ph as RAFT agent and AIBN as initiator in THF. The molecular weight of P4VP block was controlled by the feed ratio of 4VP to PS−SC(S)Ph and the conversion. But the polymerization in cyclohexane levels off at about 5 h in the plots of 4VP conversion and molecular weight of the P4VP block against polymerization time shown in Figure 1B. The initial polymerization rate (0.164 mol L^{-1} h^{-1}) is relatively higher, and after around 5 h, the polymerization rate (0.0024 mol L^{-1} h^{-1}) slowed down suddenly. This may reflect the change of polymerization mechanism at this point. Consider that the THF is a good solvent for both PS and P4VP, and cyclohexane is a solvent for PS but is a nonsolvent for P4VP. We can presume that the block polymerization in THF might display the same behavior as the RAFT polymerization of St in THF, and the turning point in Figure 1B for the polymerization in cyclohexane may be related to the aggregation of block copolymers. The formation of block copolymers in the latter case was confirmed by their ^{1}H NMR spectra (Figure 2) and GPC curves (Figure 3). Figure 2 shows the characteristic signals of P4VP at δ = 8.3 ppm and that of PS at δ = 6.6 and 7.1

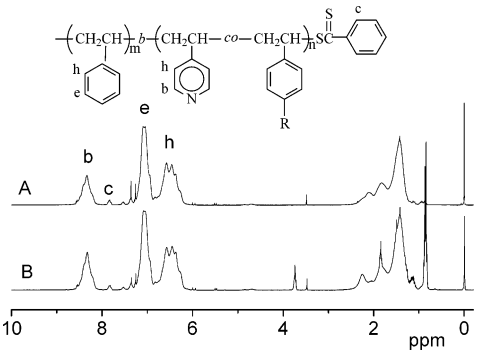

Figure 2. ^{1}H NMR spectra of the resultant block copolymers obtained from reversible addition−fragmentation transfer block polymerization of 4-vinylpyridine in cyclohexane (5 mL) at 90 °C using PS−SC(S)Ph (PS2 in Table 1) as transfer agent at different polymerization times. A: 3 h; B: 10 h. Feed molar ratio: PS−SC(S)Ph(PS2 in Table 1)/4VP/AIBN = 11/654/1.

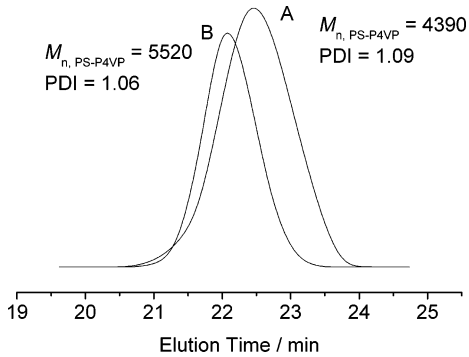

Figure 3. Gel permeation chromatography traces of block copolymers, polystyrene (PS)-*b*-poly(4-vinylpyridine) (P4VP), obtained from polymerization in cyclohexane (5 mL) at 90 °C. A: polymerized for 3 h; B: polymerized for 10 h. Feed molar ratio: PS−SC(S)Ph(PS2 in Table 1)/4VP/AIBN = 11/654/1.

ppm. On the basis of their integration ratio, the compositions of block copolymers obtained from 3 and 10 h polymerizations are poly[(4VP)$_{18}$-*b*-S$_{27}$] and poly[(4VP)$_{24}$-*b*-S$_{27}$], respectively. Unimodal and symmetrical GPC traces in Figure 3 demonstrate that those copolymers are not a mixture of the two polymers. Therefore, the micelles might be formed by microphase separation when the chain length of P4VP block increases to a critical value; the composition of the block copolymer was (4VP)$_{21}$-*b*-S$_{27}$ in the case of Figure 1B. Subsequent polymerization in the cores of micelles will be slow. This will be explained further.

RAFT Copolymerization of 4VP and DVB in Cyclohexane. To examine further the effect of solvents on the polymerization of 4VP and DVB (less than 10% relative to 4VP), the RAFT copolymerizations of 4VP and DVB with the feed molar ratio of PS−SC(S)Ph (M_n(GPC) = 2840, PDI = 1.05)/4VP/DVB/AIBN = 0.2/12/0.39/0.02 were carried out in THF and in cyclohexane, respectively. After polymerization at 90 °C in THF for 5 h, gelation occurred. However, the polymerization in cyclohexane was transparent throughout the polymerization, and at last, the polymerization solution displayed faint blue opalescence, indicating the formation of nanosized microspheres. The different phenomena between polymerizations in THF and in cyclohexane infer the difference of their polymerization mechanisms. For understanding the polymerization mechanism, we used ^{1}H NMR and GPC methods to follow the polymerization, the relationship of 4VP conversion (calculated based on NMR data), and the molecular weights; $M_{w,polymer}$(LLS) of the polymers obtained with polymerization time is shown in Figure 4. The $M_{w,polymer}$(LLS)s were determined on GPC with a multiangle laser light scattering device as

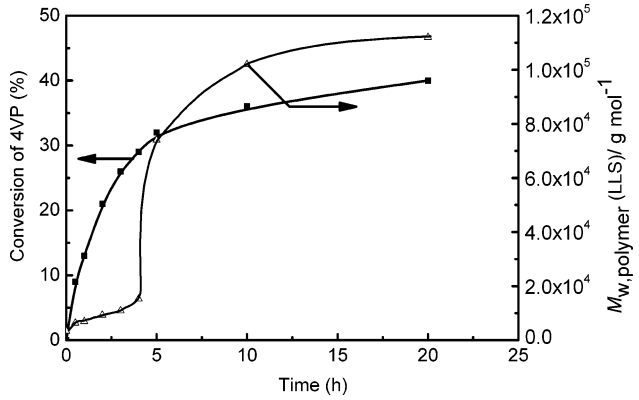

Figure 4. Relationship of 4-vinylpyridine (4VP) conversion and weight-average molecular weight, $M_{w,polymer}$(LLS) (measured on a multiangle laser light scattering device), with polymerization time for the RAFT polymerization of 4VP and divinylbenzene (DVB) with the feed molar ratio of PS−C(S)Ph ($M_{n,GPC}$ = 2840, M_w/M_n = 1.05)/4VP/DVB/AIBN = 0.2/12/0.39/1 at 90 °C in 5 mL of cyclohexane.

detector. A turning point on the two curves at around 5 h is also observed. For the plot of conversion against polymerization time shown in Figure 4, the initial polymerization rate, R_p, was 0.138 mol L^{-1} h^{-1}, and then the polymerization rate decreased (R_p = 0.0085 mol L^{-1} h^{-1}). The same phenomenon with the block copolymerization in cyclohexane was observed. This indicates that the variation of polymerization mechanism exists also. Different from slow increase of molecular weight in the linear block copolymerization observed in Figure 1B, there is a sharp increase in molecular weight at about 5 h in Figure 4. The possible reason is the aggregation of diblock copolymer, PS-*b*-(P4VP-*co*-PDVB), to form micelles with P4VP-*co*-PDVB as core and PS as shell since the P4VP is not dissolved in cyclohexane. The aggregation must occur at a critical chain length of P4VP-*co*-PDVB block in the block copolymers. The composition of the block copolymer formed at 5 h polymerization calculated on the basis of ^{1}H NMR data is poly[$(4VP)_{17}$-*b*-S_{27}]. In comparison with the composition of block copolymer obtained from RAFT block polymerization of 4VP, the critical chain length of P4VP block is slightly shorter; probably the cross-linking reactions promote the micellization at early stage of block polymerization.

To confirm further the formation of micelles at around 5 h polymerization, the GPC and MALLS analysis was used to follow the RAFT polymerization with the same feed ratio and conditions in Figure 4; the size of the polymer microspheres obtained at different times is shown in Figure 5. The polymers obtained before 4 h were too small to be detected correctly, and the big increase of the polymer size obtained at 5 h can be clearly seen in Figure 5, which should be resulted from aggregation of many macromolecules. The formation of micelles will be further confirmed later. With the progress of polymerization, the size of microspheres increased from 5.3 nm at 4 h to 17.0 nm at 20 h polymerization (Figure 5). The formation and growth process of micelles can be briefly depicted in Scheme 1. Initially, the block copolymerization of 4VP and DVB in the presence of PS−SC(S)Ph proceeded homogeneously via RAFT process, and the block copolymers with low chain length of P4VP-*co*-PDVB formed are still soluble in cyclohexane (A and B in Scheme 1). The variation of GPC traces with the evolution of polymerization in Figure 6 shows clearly the growth of block copolymers. Before 4 h, the GPC curves display two peaks: the one at the lower molecular weight position is the block copolymer, PS-*b*-P(4VP-*co*-DVB), formed, and other at higher molecular weight position is the coupling products of

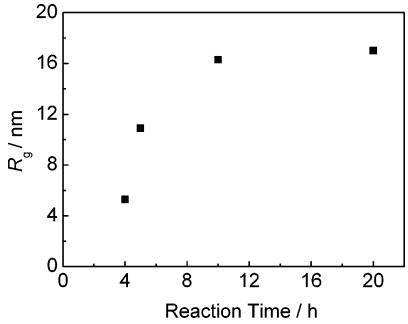

Figure 5. Variation of the radius of gyration (R_g) with polymerization time. The feed molar ratio of PS−C(S)Ph ($M_{n,GPC}$ = 2840, M_w/M_n = 1.05)/4VP/DVB/AIBN = 0.2/12/0.39/1; temperature: 90 °C; cyclohexane: 5 mL. (The molecular weight, $M_{n,GPC}$, and molecular weight distribution, M_w/M_n, were obtained from GPC measurements; 4VP = 4-vinylpyridine, DVB = divinylbenzene, AIBN = 2,2′-azobis(isobutyronitrile).)

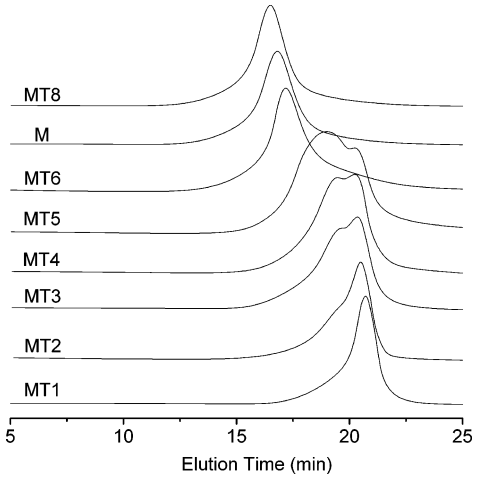

Figure 6. Gel permeation chromatography traces of the resultant core cross-linked micelles obtained from reversible addition−fragmentation transfer polymerization at different polymerization times: 0.5 h (MT1); 1 h (MT2); 2 h (MT3); 3 h (MT4); 4 h (MT5); 5 h (MT6); 10 h (M); 20 h (MT8). The feed molar ratio of PS−C(S)Ph ($M_{n,GPC}$ = 2840, PDI = 1.05)/4VP/DVB/AIBN = 0.2/12/0.39/1. (The molecular weight, $M_{n,GPC}$, and molecular weight distribution, M_w/M_n, were obtained from GPC measurements; 4VP = 4-vinylpyridine, DVB = divinylbenzene, AIBN = 2,2′-azobis(isobutyronitrile); temperature: 90 °C; cyclohexane: 5 mL.)

Scheme 1. Formation of Nanosized Micelles and Reversible Addition−Fragmentation Transfer Polymerization in This Nanospace (4VP = 4-Vinylpyridine; DVB = Divinylbenzene; AIBN = 2,2′-Azobis(isobutyronitrile))

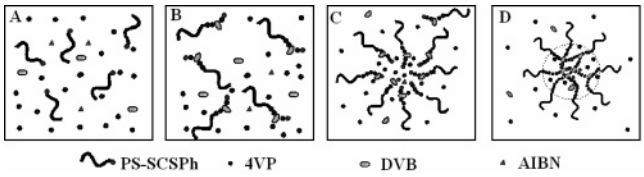

two or three PS block copolymer chains via reactions of the chain radicals with their pendent vinyl groups. With the progress of polymerization, the former peak decreases and the latter peak increases. At 4 h polymerization (MT5 in Figure 6), these two soluble copolymers are predominant in the system. At the same time the latter peaks (MT1 to MT5 in Figure 6) are shifted toward high molecular weight direction gradually with the proceeding of polymerization. When the P4VP-*co*-PDVB block grows to a critical chain length, the aggregation of the macromolecules will be taken place to form micelles (C in Scheme 1). This process can be evidenced by comparison of

GPC traces of the polymers formed at 4 and 5 h. At 5 h polymerization, the dual peak disappeared almost completely, and a new peak with tail appeared at high molecular weight position. The reasonable explanation is that the aggregation of the macromolecules formed produces micelles with cross-linked core. At this point, except that the polymerization occurs mainly in the nanosized micelles, the solution polymerization cannot be excluded because the linear block copolymer chains exist in solution still, which is evidenced by the lower molecular weight tail in the MT6 curve of Figure 6; they will continue to propagate until all the linear block polymer chains are connected to the micelles (D in Scheme 1). After 10 h, the M and MT8 traces of Figure 6 show only a single and symmetrical GPC curve. This phenomenon is different from the RAFT polymerization of DVB with macro-RAFT agent for preparation of star-shaped polymers, in which a significant amount of linear polymers was presented even after 48 h polymerization.[25,26] In the present polymerization system, all the linear block copolymers formed from the RAFT polymerization in cyclohexane will aggregate to form the micelles at last. The propagation and cross-linking reactions in the cores of micelles will avoid the cross-linking reactions between the linear polymer chains and/or among the micelles. Therefore, the formation of micelles at an appropriate polymerization time is a key to avoid gelation.

On the basis of the above discussion, two stages of polymerization as shown in Figure 1B and Figure 4 can be explained as follows. At initial polymerization, the initiation and propagation reactions underwent homogeneously; the higher polymerization rate (R_p = 0.138 mol L^{-1} h^{-1}) was observed. After 5 h polymerization, the micelles were formed, the propagation and cross-linking reactions have taken place in the cores of nanosized micelles, and the polymerization displayed low rate (R_p = 0.0085 mol L^{-1} h^{-1}). Several reasons are responsible for the low polymerization rate: (1) low 4VP concentration in the micelles formed, (2) no dithiobenzoate group in the micelles and complete consumption of AIBN, (3) restriction of monomer diffusion into micelles, and (4) too high concentration of chain transfer agent, dithiobenzoate groups in the core of micelles. For finding out the exact reasons, we did a series of experiments. First, we analyzed the concentration of monomers in micelles and in solution. After the RAFT polymerization in cyclohexane with the same feed ratio mentioned above (PS−SC(S)Ph (M_n-(GPC) = 2840, PDI = 1.05)/4VP/DVB/AIBN = 0.2/12/0.39/0.02) at 90 °C for 10 h, some of the polymerization solution was taken for the measurement of the ^{1}H NMR spectrum, and the residue was cooled to room temperature very fast in ice water, resulting in quick precipitation of the micelles. The upper clear liquid was poured out for ^{1}H NMR measurement. The micelles obtained by filtration were washed with petroleum ether (30−60 °C), and the dried micelles were used for next tests. The ^{1}H NMR spectrum of the liquid after precipitation of micelles in Figure 7B shows no signal ascribed to soluble block copolymers and a very small amount of linear PS, except signals of 4VP, DVB, and cyclohexane. Figure 7A is the ^{1}H NMR spectrum of the polymerization solution after 10 h polymerization. We can see the characteristic signals of PS and P(4VP-*co*-DVB), except characteristic signals of 4VP, DVB, and cyclohexane. On the basis of the integration ratio of signals of 4VP and DVB at δ = 8.55 and 5.22 ppm to signals of cyclohexane at δ = 1.44 ppm, we can calculate the monomer concentration (0.43 mol L^{-1}) in solution; the average concentration of the monomers in the polymerization system after 10 h was 0.62 mol L^{-1}. Comparison of these two monomer concentrations can deduce that the micelles are rich in monomers,

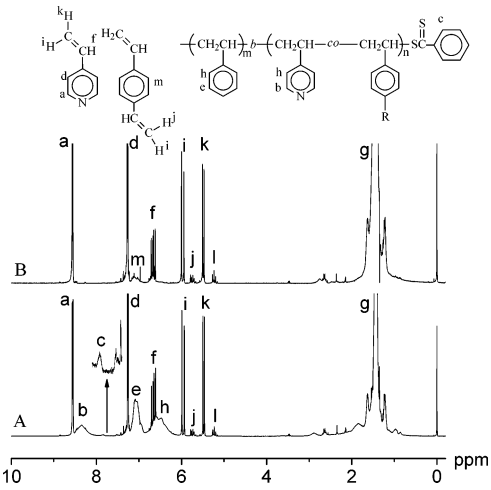

Figure 7. (A) ^{1}H NMR spectrum of the polymerization solution obtained from the reversible addition−fragmentation transfer polymerization with feed molar ratio of PS−SC(S)Ph ($M_{n,PS}$ = 2840 g mol^{-1}, M_w/M_n = 1.05)/4VP/DVB/AIBN = 0.2/12/0.39/0.02 at 90 °C for 10 h. (B) ^{1}H NMR spectrum of the solution after the polymer micelles were separated from the polymerization solution in (A).

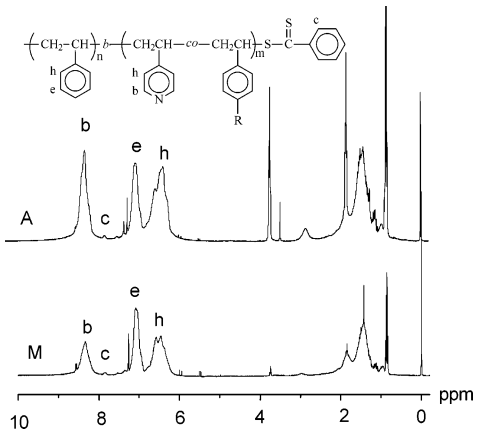

Figure 8. M: ^{1}H NMR spectrum of the micelles obtained from 10 h polymerization: Temperature: 90 °C; solvent: cyclohexane. Feed ratio: PS−SC(S)Ph ($M_{n,PS}$ = 2840 g mol^{-1}, M_w/M_n = 1.05)/4VP/DVB/AIBN = 200/400/40/1(weight ratio). A: ^{1}H NMR spectrum of the micelles separated from the polymerization solution. Polymerization of 4VP (0.2 g) in 2 mL of THF in the presence of AIBN (1 mg) and the core cross-linked micelles M (0.2 g) at 90 °C for 10 h.

which is favorable to the RAFT polymerization. Thus, the slow polymerization rate is not due to low concentration of monomers in micelles. The signal of two *o*-phenyl protons in dithiobenzoate group at δ = 7.83 ppm appears in Figure 8M of the ^{1}H NMR spectrum of micelles obtained, demonstrating the existence of the dithiobenzoate group. If high concentration of dithiobenzoate group in the compact core of micelles induces the slow polymerization rate, the polymerization of 4VP in good solvent and in the presence of cross-linked micelles should display fast polymerization rate because the core expansion of micelles will reduce the concentration of dithiobenzoate group. Therefore, the core cross-linked micelles mentioned above were added into the THF (2 mL) solution containing 4VP (0.2 g) and AIBN (0.2 g), and then the polymerization was carried out at 90 °C for 10 h. High content of 4VP units in the micelles was found from its ^{1}H NMR spectrum of micelles (Figure 8A). On the basis of the integration ratio of the signal of 4VP unit at δ = 8.34 ppm to that of St unit at δ = 7.06 ppm in Figure 8A and Figure 2B, we can find that the polymerization rate in THF is much higher than that of block copolymerization of 4VP in cyclohexane using PS−SC(S)Ph as a macro-RAFT agent. But

Table 2. Synthesis of Micelles with Different Macromolecular Chain Transfer Agent (PS−SC(S)Ph)[a]

	$M_{n,PS}$ (g mol^{-1})	$M_{n,P4VP}$(NMR)[b] (g mol^{-1})	conv (%)[c]	M_w/M_n[d]	$M_{n,P4VP}/M_{n,PS}$	R_g (nm)[e]
ML1	2000	1250	37	1.08	0.625	11
M	2840	2020	36	1.09	0.711	16.3
ML4	8400	4500	27	1.43	0.536	23
ML5	11000	5250	24	1.61	0.477	26.5

[a] PS−SC(S)Ph/4VP/DVB/AIBN = 200/400/40/1 (weight ratio); cyclohexane: 5 mL; T = 90 °C, reaction time = 10 h. [b] Determined by ^{1}H NMR data. [c] Conversionwere calculated based on the gravimetric method: conv (%) = $(W_m - W_S)/(W_{4VP} + W_{DVB}) \times 100\%$, where W_m is the weight of micelles; W_S, W_{4VP}, and W_{DVB} are the weights of PS, 4VP, and DVB, respectively. [d] Obtained from GPC measurements. [e] Determined by MALLS.

this experiment cannot exclude the contribution of fast diffusion rate in the expansion core of micelles to fast polymerization rate. For examination of diffusion on the polymerization rate, we did the same RAFT polymerization using cyclohexane as solvent instead of THF. After the polymerization at 90 °C for 10 h, a large quantity of homopolymer, P4VP was separated from the polymerization system. This demonstrates that the linear P4VP chain radicals and/or initial radicals were not easy to diffuse into the cores of micelles due to the shrinkage of P4VP-*co*-PDVB core, and the polymerization occurred mainly in the solution. But consider the competition polymerizations in solution and in the cores of micelles; the retardation function due to high concentration of dithiobenzoate group in the cores of micelles will be favorable to the formation of P4VP in solution. On the basis of the experiment facts obtained at present, we cannot identify which one of the two factors, restriction of the diffusion and high concentration of dithiobenzoate group in the cores of micelles, is responsible for the slow polymerization rate after the formation of micelles. Possibly, it is the result of these two factors.

Effect of Molecular Weight of Macro-RAFT Agent, PS−SC(S)Ph, on the Polymerization. Macro-RAFT agents with various molecular weights will form micelles with various thickness corona during the polymerization of St and DVB in cyclohexane. The thicker corona might influence the diffusion of monomers, initiator, and linear chain radicals into the core of micelles. Thus, the RAFT polymerization of 4VP and DVB using PS−SC(S)Ph with various molecular weights in cyclohexane was investigated. The conditions and results are listed in Table 2. With the increase of molecular weight of macro-RAFT agent, the monomer conversion tends to decrease. Probably thicker corona makes the diffusion more difficult. But for the chain length of the P(4VP-*co*-DVB) block formed, the opposite phenomenon was observed. A probable reason is that the critical chain length of P(4VP-*co*-DVB) block at the phase separation becomes longer with the molecular weight increase of macro-RAFT agent. As a result, the size of the micelles formed became bigger for the application of higher molecular weight macro-RAFT agent (Table 2).

Effect of Feed Ratio of 4VP/DVB on RAFT Polymerization in Cyclohexane. In the successful preparation of star-shaped polymers by the arm-first method, the amount of DVB used is an important factor. Thus, we studied the feed ratio of 4VP/DVB on the RAFT polymerization in cyclohexane. The conditions and results are listed in Table 3. Similar to the polymerization mechanism proposed in synthesis of star-shaped polymers,[3] the initial polymerization of DVB formed linear polymer, further linking and cross-linking reactions yield star-shaped polymers. The similar reactions should occur in the RAFT polymerization of 4VP and DVB in selective solvents. As shown in Scheme 2, initial RAFT polymerization of 4VP and DVB with PS−SC(S)Ph as macro-RAFT agent afforded the linear block copolymers, PS-*b*-P(4VP-*co*-4VP). When much DVB was used, the linear P(4VP-*co*-DVB) blocks formed initially contain more DVB units; cross-linking reactions have taken place early, forming small sized micelles. Thus, the R_g decreases with feed ratio increase of DVB to 4VP (Table 3). Since the micelles were formed via microphase separation at the early stage of polymerization, and the polymerization in micelles had lower polymerization rate, it is reasonable that the conversions in the same polymerization time decreased with the content increase of DVB in the mixture of 4VP and DVB.

Table 3. Synthesis of Micelles from Different DVB Feeding Ratios[a]

	DVB (g)	$M_{n,P4VP}$(NMR)[b] (g mol^{-1})	conv (%)[c]	M_w/M_n[d]	$M_{n,P4VP}/M_{n,PS}$	R_g (nm)[e]
M	1.2	2020	36	1.09	0.711	16.3
MC2	1.8	1990	35	1.17	0.701	16.4
MC3	2.4	1560	24	1.04	0.549	11.4
MC4	3.6	1290	23	1.10	0.454	8.1

[a] Feed weight ratio of PS−SC(S)Ph/4VP/AIBN = 200/400/1; $M_{n,PS}$ of PS−SC(S)Ph = 2840 g mol^{-1}; cyclohexane: 5 mL; T = 90 °C; reaction time = 10 h. [b] Determined by the ^{1}H NMR method. [c] Conversions were calculated based on the gravimetric method: conv (%) = $[(W_m - W_S)/(W_{4VP} + W_{DVB})] \times 100\%$, where W_m is the weight of micelles; W_S, W_{4VP}, and W_{DVB} are the weights of PS, 4VP, and DVB, respectively. [d] Obtained from GPC measurements. [e] Determined by MALLS.

Scheme 2. Preparation of Micelles by Polymer Linking Reaction

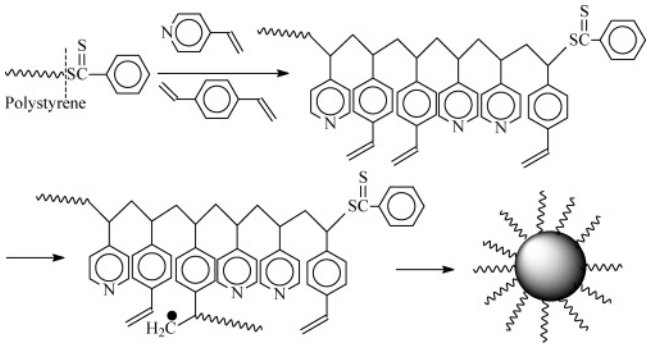

Characterization of Micelles. For verifying the formation of micelles obtained from the RAFT copolymerization in selective solvent, two samples, Sam10 and Sam 20, were prepared by RAFT copolymerization respectively from PS−SC(S)Ph with M_n(GPC) = 3550, M_w/M_n = 1.04 (Sam10) and M_n(GPC) = 11 700, M_w/M_n = 1.03 (Sam20). The preparation conditions and results are listed in Table 4. The DLS and SLS studies of the resultant Sam10 and Sam20 in THF solution as shown in Figure 9 verified the formation of micelles, and their average hydrodynamic radius $\langle R_h \rangle$ is 16.4 nm for Sam10 and 22.0 nm for Sam20. The relatively low polydispersity indexs (μ_2/Γ^2) values (0.08 and 0.09) listed in Table 4 indicate narrow size distributions of these two micelles obtained. Those micelles are spherical because the average characteristic line widths (Γ/q^2) are independent of the angle of detection (inset of Figure 9). Since the two blocks PS and P4VP can dissolve in THF, the narrowed spherical nanosize particles observed in THF solution confirm stability of the two micelles. The values of the R_g/R_h ratio listed in Table 4 can be used to characterize their morphology.[27,28] Generally, those nanoparticles with R_g/R_h ratios = 0.774 are thought as uniform and nondraining spheres, much higher R_g/R_h ratios of Sam10 and Sam20 than 0.774 indicate that the two samples have a loose structure corresponding to lower cross-linking degree of the core, and

Table 4. Characterization Data of the Core Cross-Linked Micelles Prepared by the RAFT Polymerization of 4VP and DVB Using PS−SC(S)Ph as Macro-RAFT Agent

	feed molar ratio										
	PS−SC(S)Ph[a]	4VP	DVB	AIBN	conv[b] (%)	M_w[c] (g mol^{-1})	$\langle R_h \rangle$ (nm)	$\langle R_g \rangle / \langle R_h \rangle$	ρ (g/cm^3)[d]	μ_2/Γ^2	N_{agg}[e]
Sam10	1	61	3.6	0.14	48.5	1.80×10^6	16	1.29	0.162	0.08	226
Sam20	1	117	7.2	0.28	30.1	2.97×10^6	22	1.22	0.141	0.09	193

[a] For Sam10, PS−SC(S)Ph: M_n(GPC) = 3550, M_w/M_n = 1.04; For Sam20, PS−SC(S)Ph: M_n (GPC) = 11 700, M_w/M_n = 1.03; cyclohexane: 6 mL; temperature: 90 °C; polymerization time: 10 h. [b] Conversions were calculated based on the gravimetric method: conv (%) = $[(W_m - W_S)/(W_{4VP} + W_{DVB})] \times 100\%$, where W_m is the weight of micelles; W_S, W_{4VP}, and W_{DVB} are the weights of PS, 4VP, and DVB, respectively. [c] Measured by static light scattering. [d] ρ was calculated according to $\rho = (M_w/N_A)/(4\pi R_h)^3/3)$. [e] N_{agg} was calculated according to $N_{agg} = M_w/M_{w,single\ arm} = M_w/(M_{w,PS} + M_{w,P4VP})$.

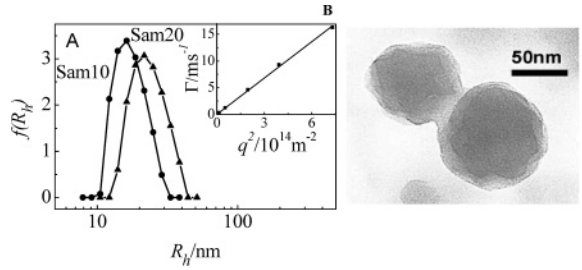

Figure 9. (A) Hydrodynamic radius distributions of the micelles with cross-linked cores in THF measured by the dynamic light scattering method. The inset shows that Γ/q^2 is independent of the angle of detection. (B) TEM photo of the core cross-linked micelles (Sam10).

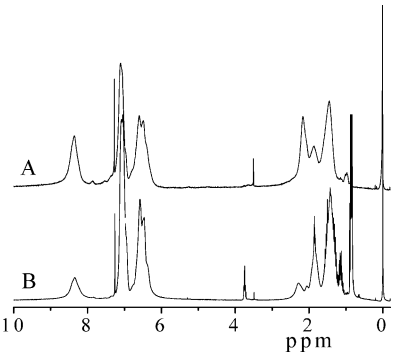

Figure 10. ^{1}H NMR spectra of (A) the core cross-linked micelles PS_{36}-*b*-$P4VP_{33}$ obtained from RAFT polymerization of 4VP and DVB using PS−SC(S)Ph with M_n(GPC) = 3550, M_w/M_n = 1.04 as macro-RAFT agent and (B) PS_{117}-*b*-$P4VP_{37}$ using PS−SC(S)Ph with M_n(GPC) = 11 700, M_w/M_n = 1.03 as macro-RAFT agent. Solvent: $CDCl_3$.

both the core and the shell were hydrodynamically draining in THF solvent.[29] Zimm plots yielded molar masses of approximately 1.80×10^6 and 2.97×10^6 g mol^{-1}, and the corresponding arm numbers of the micelles, N_{agg}, are 226 for Sam10 and 193 for Sam20 (Table 4).

We call the synthetic products in this study as micelles, not star polymers, because the cores are quite bigger in comparison with the coronas of micelles. An evidence for loose cores is the R_g/R_h ratio as we mentioned; other evidence is the ^{1}H NMR spectra shown in Figure 10. When the cores are highly cross-linked, those proton signals belonging to the core polymers will not appear in the ^{1}H NMR spectrum. However, ^{1}H NMR spectra in Figure 10 show clearly the characteristic signals of both PS and P4VP blocks: the phenyl proton signals of PS block at δ = 7.1 and 6.6 ppm and the pyridine proton signals of P4VP at δ = 8.32 and 6.44 ppm. From their integration ratio, we can calculate the compositions of two polymer micelles, PS_{36}-*b*-$P4VP_{33}$ for Sam10 and PS_{117}-*b*-$P4VP_{37}$ for Sam20, which are consistent with the corresponding values calculated from the initial ratio of 4VP and DVB to PS macro-RAFT agent and conversion. This indicates fully stretching of P4VP/DVB block chain in the cores of micelles in $CDCl_3$.

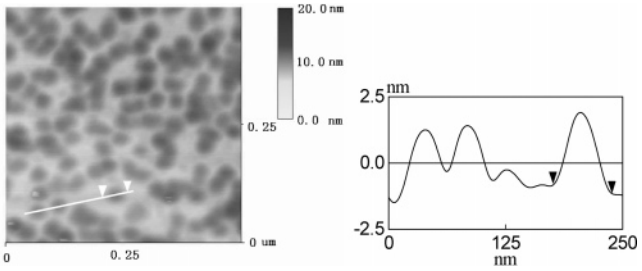

Figure 11. AFM images and section analysis of micelles from Sam10.

The micelles with P4VP/DVB core and PS as shell can be observed directly from their TEM photos. Figure 9B is a typical TEM photo of the dried micelles made from Sam10. The spherical particles with dark cores and bright shells can be clearly seen, and the average diameters of the micelles and dark cores are around 78 and 62 nm, respectively. The micelle size is substantially larger than the $2R_h$ value (32 nm) in THF; one probable reason is that the micelles with loosely cross-linked cores are deformed during the evaporation of solvents. Similar results were achieved by AFM observation (Figure 11); the height of the particles is only 3.1 nm, substantially smaller than of the diameter values, suggesting the loose structure of the particles and great deformation during the process of solvent evaporation.

Conclusion

The RAFT polymerizations of 4VP and/or DVB in solvent and nonsolvent of poly(4VP-*co*-DVB) with macro-RAFT agent display different kinetic behaviors: for polymerization in THF, one polymerization rate and almost linear increase of $M_{n,P4VP}$-(NMR) with polymerization time in the block polymerization of 4VP, but the formation of gelation in the copolymerization of 4VP and DVB (less than 10% relative to 4VP); for polymerization in cyclohexane, appearance of a turn point at around 5 h on the curves of conversion and $M_{n,P4VP}$(NMR) against polymerization time in the block polymerization of 4VP, however, sudden decrease of polymerization rate (from R_p = 0.138 to R_p = 0.0085 mol L^{-1} h^{-1}) and sharp increase of $M_{w,polymer}$ at around 5 h in the copolymerization of 4VP and DVB. The variations at around 5 h polymerization in cyclohexane are due to the formation of micelles (less than 50 nm) with PS as shell and poly(4VP-*co*-DVB) as core induced by microphase separation. The RAFT polymerization before 5 h forms soluble block copolymers, and when the chain length of poly(4VP-*co*-DVB) increases to a critical value (poly[$(4VP)_{17}$-*b*-St_{27}] for PS2 in Table 1), the phase separation will occur to form micelles. After the formation of micelles, the polymerization takes place in the nanosized micelles, which will avoid the formation of gel. The higher molecular weight of macro-RAFT agent will lead to the formation of larger size of micelles, but the higher content of DVB in the mixture of 4VP and DVB will yield the micelles with small size. The slow polymerization rate after 5 h polymerization may be attributed to the restriction

of diffusion and high concentration of dithiobenzoate group in the cores of micelles. This provides another easy route to synthesize core cross-linked micelles. In comparison with the micelles synthesized by self-assembling of block and graft copolymers, the advantages are the block copolymerization, micellization, and core cross-linking reaction in one pot and the resultant higher concentration of the micelles up to 30% w/w.

Acknowledgment. This work is supported by the National Natural Science Foundation of China under Contracts 20374048 and 20234020.

References and Notes

(1) Mishra, M. K. *Macromolecular Engineering: Recent Advances*; Plenum Press: New York, 1995.
(2) Hadjichristidis, N.; Pitsikalis, M.; Pispas, S.; Iatrou, H. *Chem. Rev.* **2001**, *101*, 3747−3792.
(3) Baek, K.; Kamigaito, M.; Sawamoto, M. *Macromolecules* **2001**, *34*, 215−221.
(4) Tsoukatos, T.; Pispas, S.; Hadjichristidis, N. *J. Polym. Sci., Part A: Polym. Chem.* **2001**, *39*, 320−325.
(5) Zhang, X.; Xia, J.; Matyjaszewski, K. *Macromolecules* **2000**, *33*, 2340−2345.
(6) Bosman, A.; Heumann, A.; Klaerner, G.; Benoit, D.; Frechet, J.; Hawker, C. *J. Am. Chem. Soc.* **2001**, *123*, 6461−6462.
(7) Du, J.; Chen, Y. *J. Polym. Sci., Part A: Polym. Chem.* **2004**, *42*, 2263−2271.
(8) Baek, K.; Kamigaito, M.; Sawamoto, M. *Macromolecules* **2002**, *35*, 1493−1498.
(9) Riess, G. *Prog. Polym. Sci.* **2003**, *28*, 1107−1170.
(10) Weberskirch, R.; Preuschen, J.; Spiess, H. W. *Macromol. Chem. Phys.* **2000**, *201*, 995−1007.
(11) Kakizawa, Y.; Harada, A.; Kataoka, K. *J. Am. Chem. Soc.* **1999**, *121*, 11247−11248.
(12) Weaver, J.; Tang, Y.; Liu, S.; Iddon, P.; Grigg, R.; Billingham, N.; Armes, S.; Hunter, R.; Rannard, S. *Angew. Chem., Int. Ed.* **2004**, *43*, 1389−1392.
(13) Zhang, L.; Eisenberg, A. *Science* **1995**, *268*, 1728−1731.
(14) Antonietti, M.; Goltner, C. *Angew. Chem., Int. Ed.* **1997**, *36*, 910−928.
(15) Checot, F.; Lecommandoux, S.; Gnanou, Y.; Klok, H. *Angew. Chem., Int. Ed.* **2002**, *41*, 1339−1343.
(16) Meric, P.; Yu, K.; Tsang, S. *Catal. Lett.* **2004**, *95*, 39−43.
(17) Guo, A.; Liu, G.; Tao, J. *Macromolecules* **1996**, *29*, 2487−2493.
(18) Topp, M.; Dijkstra, P.; Talsma, H.; Feijen, J. *Macromolecules* **1997**, *30*, 8518−8520.
(19) Topp, M.; Leunen, I.; Dijkstra, P.; Tauer, K.; Schellenberg, C.; Feijen, J. *Macromolecules* **2000**, *33*, 4986−4988.
(20) Semagina, N.; Joannet, E.; Parra, S.; Sulman, E.; Renken, A.; Kiwi-Minsker, L. *Appl. Catal., A* **2005**, *280*, 141−147.
(21) Seregina, M.; Bronstein, L.; Platonova, O.; Chernyshov, D.; Valetsky, P.; Hartmann, J.; Wenz, E.; Antonietti, M. *Chem. Mater.* **1997**, *9*, 923−931.
(22) Semagina, N.; Bykov, A.; Sulman, E.; Matveeva, V.; Sidorov, S.; Dubrovina, L.; Valetsky, P.; Kiselyova, O.; Khokhlov, A.; Stein, B.; Bronstein, L. *J. Mol. Catal. A: Chem.* **2004**, *208*, 273−284.
(23) Goto, A.; Sato, K.; Tsujii, Y.; Fukuda, T.; Moad, G.; Rizzardo, E.; Thang, S. *Macromolecules* **2001**, *34*, 402−408.
(24) Li, Y.; Shi, P.; Zhou, Y.; Pan, C. *Polym. Int.* **2004**, *53*, 349−354.
(25) Zheng, G.; Pan, C. *Polymer* **2005**, *46*, 2802−2810.
(26) Lord, H.; Quinn, J.; Angus, S.; Whittaker, M.; Stenzel, M.; Davis, T. *J. Mater. Chem.* **2003**, *13*, 2819−2824.
(27) Peng, H.; Chen, D.; Jiang, M. *Langmuir* **2003**, *19*, 10989−10992.
(28) Liu, S.; Billingham, N.; Armes, S. *Angew. Chem., Int. Ed.* **2001**, *40*, 2328−2331.
(29) Zhao, Y.; Hu, T.; Lv, Z.; Wang, S.; Wu, C. *J. Polym. Sci., Part B: Polym. Phys.* **1999**, *37*, 3288−3293.

MA0517897